A Linear Dynamic Model for Flexible Robotic Manipulators

Gordon G. Hastings and Wayne J. Book

ABSTRACT: The design of lightweight links for robotic manipulators results in flexible links. Accurate control of lightweight manipulators during the large changes in configuration common to robotic tasks requires dynamic models that describe both the rigid-body motions, as well as the flexural vibrations. This paper describes a linear state-space model for a single-link flexible manipulator and compares simulation of the model to measurements made on a 4-ft-long direct-drive arm.

Introduction

The model discussed in this paper forms the base for an in-depth investigation into the control of flexible manipulators [1]. One method being investigated for modeling flexible manipulators [2] relies heavily on identification of the flexible manipulator and its input/output relationships from measurements. The modeling process selected for this work depends on parameters available from the hardware design and insight into the effects of state feedback on link vibrations.

The initial sections discuss the modeling process and steps taken to verify physical parameters as well as program implementation. The latter section compares simulations of the model to experimental measurements.

Model Generation

This section describes the formation of a linear state-space model for flexible manipulators. The process of forming the model will be outlined in this section. The first step of the process is to describe the position of every point along the flexible manipulator. A linear combination of vibratory modes to describe flexible deflections and a rigid-body motion of the center of mass are selected. A manipulator with a rigid-body rotation and flexible "clamped-mass" mode is depicted in Fig. 1.

The flexible deflections are described by an infinite series of separable modes. Separability in this instance refers to describing the flexible deflections as a series of assumed modes [3], which are products of two functions, each of which is a function of a single variable: one a function of a spatial variable and the other a function of time. This is noted as

$$w(x, t) = \Sigma\, \phi_i(x) q_i(t), \quad \text{for } i = 1, 2, \cdots, n \tag{1}$$

This separability is important in later phases, when the model is formed in terms of time-varying variables only.

Next, the kinetic and potential energies are derived. The distributed character of the flexible manipulator is taken into account via integral expressions over the mass of the entire system in forming the energy expressions. The integral for calculating the kinetic energy (KE) has the following form:

$$\mathrm{KE} = \frac{1}{2} \int \dot{R} \cdot \dot{R} dm \tag{2}$$

where $\dot{R}$, the absolute velocity vector, and mass, range over the entire system. The potential energy (PE) of the system is stored in the flexible modes and can be attributed to "modal stiffnesses" K_1, which are evaluated by integrals over the length of the link, which account for bending energy.

$$K_i = \frac{1}{2} \frac{EI}{L^3} \Sigma\, q_i^2(t) \int_0^1 \left[\frac{d^2 \phi_i(\xi)}{d\xi^2} \right]^2 d\xi \tag{3}$$

Lagrange's equations of motion can be formed from the energies:

$$\frac{d}{dt} \left| \frac{\partial \mathrm{KE}}{\partial \dot{z}_i} \right| - \frac{\partial \mathrm{PE}}{\partial z_i} = Q_i \tag{4}$$

where the z_i are the coordinates and Q_1 are the generalized work terms associated with each coordinate. Turning the computational crank on the various differentials and integrals results in a coupled set of second-order dynamic equations with familiar form;

$$[M]\, \ddot{z} + [K] z = [Q] \tag{5}$$

$$z = [\theta, q_1(t), q_2(t), \cdots, q_n(t)] \tag{6}$$

Here, M is a mass matrix, K represents stiffness, and Q the input. The dynamic equations are easily organized into a state-space model, as shown in Eq. (7). The motor torque at the joint and the generalized work terms, Q_i, are related by the rotation of the joint, which occurs with each variable. Examination of the form of the model reveals the expected result that the coupling between the modes and the rigid-body motion occur from inertial terms of the mass matrix.

Equation (7) depicts a $2(n + 1)$-order linear model, where n is the number of included modes. Nonlinear terms arise from the evaluation of Eq. (2) for the kinetic energy. The model is linearized by noting that the amplitude of the vibrations is small compared to the length of the beam.

$$\begin{vmatrix} \dot{\theta} \\ \dot{q}_1 \\ \dot{q}_2 \\ \vdots \\ \ddot{\theta} \\ \ddot{q}_1 \\ \ddot{q}_2 \\ \vdots \end{vmatrix} = \begin{vmatrix} & & \\ & 0 & I \\ & & \\ & M^{-1}K & 0 \end{vmatrix} \begin{vmatrix} \theta \\ q_1 \\ q_2 \\ \vdots \\ \dot{\theta} \\ \dot{q}_1 \\ \dot{q}_2 \\ \vdots \end{vmatrix} + \begin{vmatrix} 0 \\ \\ M^{-1}Q \end{vmatrix} |u| \tag{7}$$

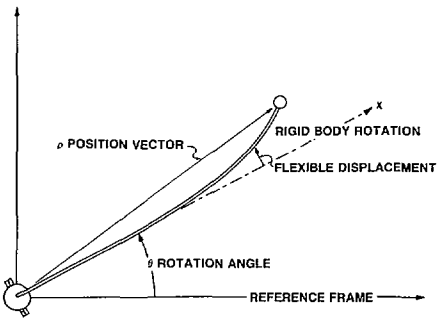

Fig. 1. Flexible manipulator.

This work was sponsored by the NASA Langley Research Center under Grant NAG-1-623, and by the National Science Foundation under Grant MEA-8303539. These results were presented at the 1986 IEEE Robotics and Automation Conference, San Francisco, California, April 7–10, 1986. Gordon G. Hastings is now with the Department of Mechanical Engineering, Clemson University, Clemson, SC 29631, and Wayne J. Book is with the School of Mechanical Engineering, Georgia Institute of Technology, Atlanta, GA 30332.

0272-1708/87/0200-0061 $01.00 © 1987 IEEE

Mode Selection and Frequency Determinant

The remaining task in generating a trial model is the selection of the flexible modes to be used in forming the constant mass and stiffness matrices.

The path chosen in this work is to select admissible functions as candidates, which are solutions to closely related problems. These solutions are eigenfunctions for selected "clamped-mass" and "pinned-mass" boundary-value problems. "Clamped" describes a boundary condition where the joint is fixed against rotation, "pinned" describes a joint with motor inertia free to rotate, and "mass" describes the condition of the payload at the other beam boundary. The admissible functions will then satisfy the differential equation, the essential or geometric boundary conditions, and the natural boundary conditions of the free-vibration problem.

Trial mode shapes were obtained by solving the differential equation for a Bernoulli-Euler beam with selected boundary conditions. The problem is formulated in terms of a frequency determinant for the determination of the eigenfunctions and associated frequencies.

Experimental Setup

This section describes the experimental system used in examining the model. The system consists of a flexible arm with payload, DC torque motor with servo-amp, signal conditioning with A/D conversion for data acquisition, 16-bit computer system for implementation of control algorithms, and D/A conversion for torque signal output.

The processor is equipped for hardware computation of floating-point operations with a characteristic time for 32-bit multiplications of 19 μsec. A torque motor is driven by a high internal gain DC servo-amp configured with a sense resistor on the motor output to act as a current source. The physical configuration of the flexible arm, torque motor, and sensors is represented in Fig. 2.

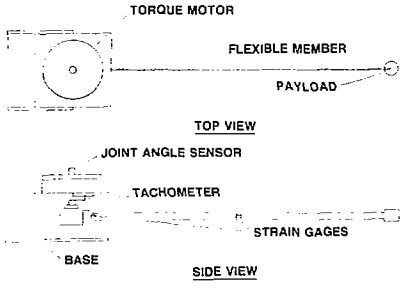

Fig. 2. Flexible beam apparatus.

Table 1 identifies the important parameters of the beam, which were used as inputs to the modeling process.

Table 1
System Parameters

Flexible Beam	
Material	Aluminum 6061-T6
Form	Rectangular, $\frac{3}{4} \times \frac{3}{16}$ in.
Length	48 in.
Moment of Inertia	4.12E-4 in.^{4}

Parameter and Program Verification

This section describes experiments conducted to verify system parameters and program implementation of the model generation process. Initially, the frequencies determined via the Bernoulli-Euler beam equations with clamped-mass and pinned-mass boundary conditions are compared to measured eigenvalues of the beam. This examines beam length, modulus, and density parameters, as well as the suitability of the chosen boundary conditions.

Figure 3 shows a measured transfer function from random torques input by the motor to strain at the base of the beam. The peaks correspond to clamped-mass modes, as the clamped boundary condition results in modes having maximum moments at the base of the beam. The valleys are associated with pinned-mass modes, as this boundary condition results in modes that have small moments, which rotate the motor inertia. Martin [4] discusses measurement zeros, which occur in flexible structures.

The vibratory modes were additionally calculated by the frequency determinant method. Table 2 compares the measured modal frequencies to those computed using the Bernoulli-Euler beam. The application of the Bernoulli-Euler formulation to the clamped-mass case agrees very well with the measured frequencies, however, the pinned-mass conditions were not as accurate.

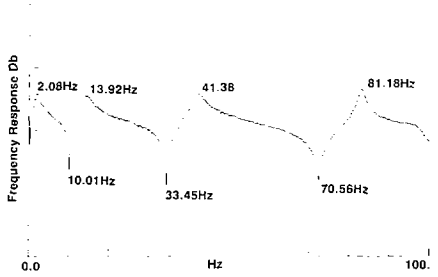

Fig. 3. Frequency response for clamped beam.

The poorer agreement for the pinned case is attributed to the friction found in the joint hardware; this is a difficult condition to model and may have a significant effect for the small-amplitude motions used during the tests.

The next step checked the model generation algorithm. Normalization of the modal masses allows the checking of the computations by examining the diagonal components of the stiffness matrix. Normally, for second-order systems, the natural frequency is the square root of the stiffness divided by the mass. Thus, the normalized stiffnesses should correspond to the squares of the modal frequencies input to the process.

A program was implemented that solved vibratory modes, calculated the mass and stiffness integrals, and computed the dynamic equations. The algorithm was checked for both the clamped-mass and pinned-mass modes. Table 3 presents a comparison of the modal frequencies input to the modeling process to the square roots of K_i. The results are very good; however, it was necessary to use higher precision computations for the higher modes.

Dynamic Response Comparison

The previous section provides confidence that the beam parameters have been properly identified and modeled by the Bernoulli-Euler beam. The computational procedure has additionally been checked. The major ques-

Table 2
Comparison of Modal Frequencies, Hz

	Clamped Mass		Pinned Mass	
Mode	Measured	Calculated	Measured	Calculated
1	2.08	2.096	10.01	9.732
2	13.92	13.989	33.45	31.608
3	41.38	41.524	70.56	62.683
4	81.18	81.225		148.768
5		136.352		216.048

Table 3
Comparison of Frequencies Determined by Stiffness Computations, Hz

Clamped Mass		Pinned Mass	
Input	Stiffness$^{1/2}$	Input	Stiffness$^{1/2}$
2.096	2.096	9.732	9.732
13.989	13.989	31.608	31.608
40.552	40.524	62.683	62.683
81.225	81.225	148.768	148.768
136.352	136.344	216.048	214.621

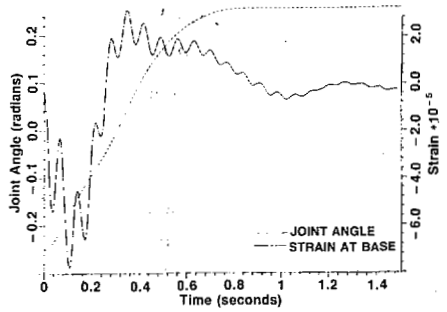

Fig. 6. Simulated response, two clamped-mass modes.

tions concerning the model can now be investigated:

- Choosing the modal candidates.
- Required model order.
- Is a linear model of the coupling adequate?

The following paragraphs describe simulations and experiments conducted to gain insight into the answers to these questions. The simplest and best understood controller for flexible arms is a *collocated controller*, that is, a control system where the measurement and actuation are located at the same point. A collocated controller was implemented for the experimental system that applied a position gain to joint angle measurements and a rate gain to angular velocity measurements.

The position gain was selected to provide the rigid-body mode with a characteristic time of 1 sec. The rate gain was selected to provide a damping ratio of 0.7. Higher gains could be selected that stress the impact of flexibility on the control strategy; however, the chosen gains provide a good starting point well within the operating parameters of the system. In addition, the system displayed linear behavior over a large range of gains.

Figure 4 displays the measured response of the experimental system to a step change in desired joint angle. Strain measurements presented in the figure, while not used in the controller, provide an indication of the relative modal amplitudes.

The dynamic model was discretized and simulated for the step angle change. Small amounts of damping (typically damping ratios ranging from 0.007 to 0.010, based on transfer function measurements using an impulse hammer as the input and strain at the base as the output [5]) were introduced into the model for the flexible modes. In addition, hysteretic joint friction was modeled as coulomb friction [6] and was included in the digital simulation. Inclusion of modal damping and hysteresis in the simulations improved the agreement of the models, especially in the time interval following the large initial transients.

Figure 5 shows the results for a model implemented with five clamped-mass modes, while Fig. 6 presents a model using two clamped-mass modes. The last case simulated used five pinned-mass modes as inputs to the modeling process. This is presented in Fig. 7.

The simulations based upon clamped-mass modes agree best with measured responses. Surprisingly, the model implemented with only two clamped-mass modes agrees almost as well as, if not better than, the higher order model. The poorer agreement of the higher order model is probably due to poor estimation of the damping by use of the impulse hammer measurements. Additional damping in the higher modes from the joint is likely when the joint is in motion. Should large-amplitude vibrations occur in the higher frequencies, as shown in Fig. 5, larger models, including the higher flexible modes, would be required. This presentation may be somewhat misleading, as better determination of damping for the higher modes could provide better results. It is apparent that a dominant portion of the response is adequately characterized by as few as two modes.

Summary and Discussion

A modeling process to generate a linear model for use in controlling flexible manipulators was presented and compared to experimental measurements for a joint angle position and rate feedback controller. The model eigenvalues agreed well with experimentally determined frequencies of the vibratory modes. Damping values implemented in the model, which were determined from clamped-mass measurements with the manipulator's joint fixed, appeared to be the major source of discrepancy in the measured transient responses. The actual responses tended to damp out faster than the prediction, indicating increased damping of the vibratory modes occurring during large manipulator motions.

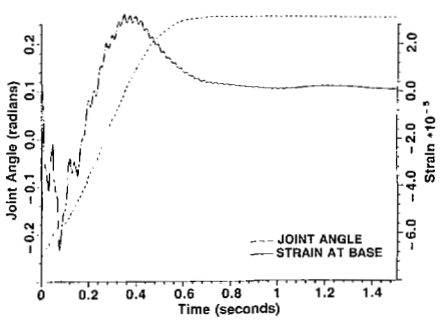

Fig. 4. Measured step response.

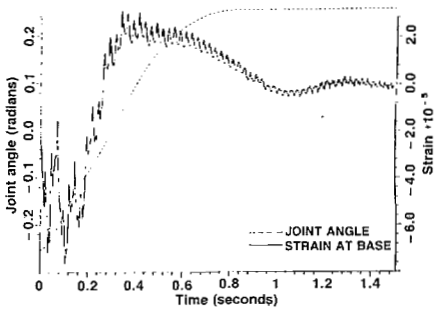

Fig. 5. Simulated response, five clamped-mass modes.

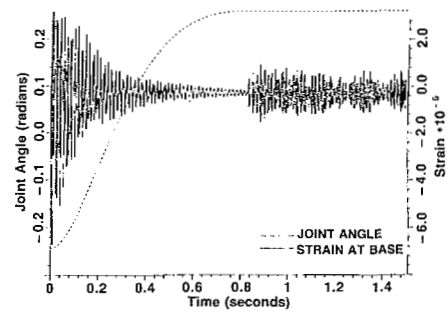

Fig. 7. Simulated responses, five pinned-mass modes.

Qualitatively, the dominant parts of the transient responses were characterized by inclusion of as few as two assumed flexible modes in the dynamic model. Future work focuses on quantifying model performance; specifically, norms of the state errors are being considered. The quantitative measures could be used to optimize model parameters or evaluate accuracy of modeling techniques and assumptions.

The selection of appropriate trial mode shapes must consider the feedback law to be implemented, as the applied torque dominates the boundary condition at the base of the link. Clamped-mass modes yielded good results for the simple collocated controller and were used extensively in later state feedback experiments [1] using the vibratory mode variables.

References

[1] G. G. Hastings, "Controlling Flexible Manipulators, An Experimental Investigation," Ph.D. thesis, School of Mechanical Engineering, Georgia Institute of Technology, Aug. 1986.

[2] E. Schmidtz, "Experiments on the End-Point Position Control of a Very Flexible One-Link Manipulator," Stanford University, Stanford, CA, SUDAAR 548, June 1985.

[3] L. Meirovitch, *Elements of Vibration Analysis*, New York: McGraw-Hill, 1975.

[4] G. D. Martin, "On Control of Flexible Systems," Ph.D. thesis, Stanford University, Stanford, CA, 1978.

[5] F. H. Chu and B. P. Wang, "Experimental Determination of Damping in Materials and Structures," *Damping Applications and Vibration Control, ASME Transactions*, AMD, vol. 38, pp. 113–122, 1980.

[6] W. T. Thompson, *Theory of Vibration with Applications*, Second Edition, Englewood Cliffs, NJ: Prentice-Hall, 1981.

Gordon G. Hastings earned the B.S. degree from Florida Atlantic University in 1978, the M.S.M.E. degree from the University of Maryland in 1983, and the Ph.D. degree from Georgia Institute of Technology in 1986. He is an Assistant Professor of Mechanical Engineering at Clemson University, Clemson, South Carolina. His research interests include dynamics, control, and mechanism design, with particular emphasis on hardware problems arising in real-time control applications. He has published several papers on real-time control experiments of flexible manipulators. Prior to pursuing his doctoral degree he acquired five years of industrial experience, primarily with Westinghouse Electric Corporation, performing research and development tasks on U.S. Navy contracts.

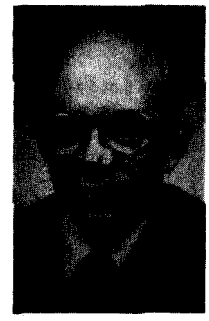

Wayne J. Book earned the B.S. degree from the University of Texas in 1969 and the Ph.D. degree from the Massachusetts Institute of Technology in 1974, both in mechanical engineering.

He is Professor of Mechanical Engineering and Director of the Computer Integrated Manufacturing Systems (CIMS) Program at the Georgia Institute of Technology, Atlanta, Georgia, where he teaches courses in control, robotics, and manufacturing automation. His research includes the dynamics, control, and design of light-weight, high-speed robot arms and flexible automation, on which he has published numerous papers and consults with industry. Under his direction, the CIMS Program has been named to receive the 1986 University LEAD Award presented by the Society of Manufacturing Engineers for excellence in education in integrated manufacturing. Dr. Book is active in ASME, serving on the Executive Committee of the Dynamic Systems and Control Division and in the IEEE, where he is an Associate Editor of the *Transactions on Automatic Control*. He is General Chairman of the 1988 American Control Conference.

Out of Control

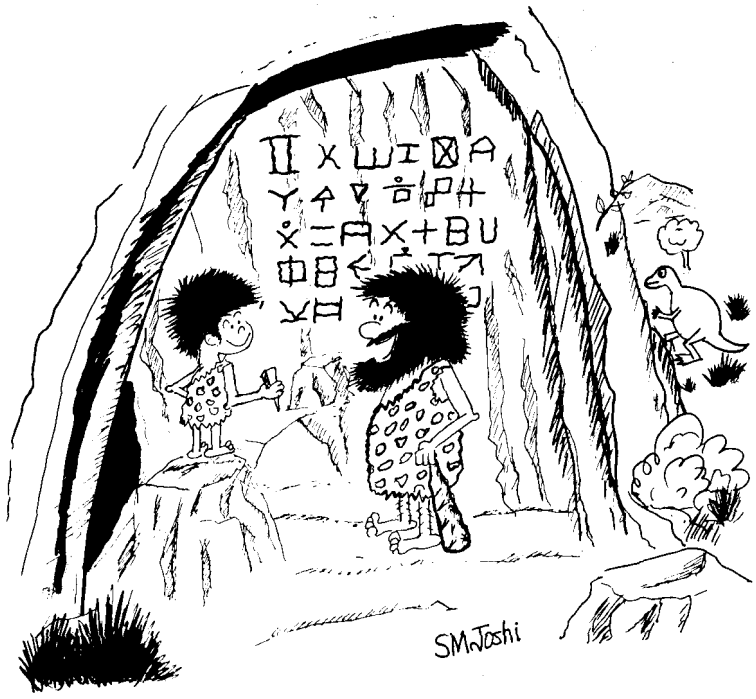

"Nice artwork, kiddo! I've got a gut feeling that a great many people will make a living off that third line someday!"